Antigene Effect in K562 Cells of a PEG-Conjugated Triplex-Forming Oligonucleotide Targeted to the *bcr*/*abl* Oncogene†

Valentina Rapozzi,‡ Susanna Cogoi,‡ Paola Spessotto,§ Angela Risso,‡ Gian Maria Bonora,|| Franco Quadrifoglio,‡ and Luigi Emilio Xodo*,‡

Department of Biomedical Sciences and Technologies, School of Medicine, Piazzale Kolbe 4, 33100 Udine, Italy, Centro di Riferimento Oncologico (CRO), Aviano, Italy, and Department of Chemical Science, University of Trieste, Via Giorgieri 1, 34127 Trieste, Italy

Received June 22, 2001; Revised Manuscript Received October 29, 2001

ABSTRACT: Triplex-forming oligonucleotides are able to modulate gene expression by site-specific binding to genomic DNA. Their use as therapeutic agents is limited by inefficient cellular uptake, scarce nuclear internalization, and oligonucleotide self-aggregation. In this study, we demonstrate that a 13-mer AG motif oligonucleotide covalently linked to a high-molecular mass (9000 Da) polyethylene glycol (PEG ODN_{13}) exhibits uptake and biological properties that are superior to those of the nonconjugated isosequence analogue (free ODN_{13}). Band-shift and footprinting experiments showed that PEG ODN_{13} forms a stable triple helix (apparent K_d between 10^{-6} and 10^{-7} M in 50 mM Tris-acetate, 10 mM $MgCl_2$, pH 7.4, 37 °C) with a natural polypurine-polypyrimidine target located in the 5′ flanking region of the human *bcr*/*abl* oncogene. Confocal laser microscopy performed on unfixed live cells stained with hexidium iodide as well as on glass-fixed cells stained with propidium iodide showed that fluorescein-labeled PEG ODN_{13} is far more efficiently taken up and internalized in the nucleus by K562 and HeLa cells than the nonconjugated free ODN_{13}. It was found that PEG ODN_{13} specifically downregulated the transcription of *bcr*/*abl* mRNA at 65 ± 5% with respect to control and inhibited cell growth by 32 ± 3% in a 3 day liquid culture assay. Moreover, PEG ODN_{13} was more resistant against S1 and fetal bovine serum nucleases than free ODN_{13}, and less inclined to self-associate into multistrand structures in solution. Taken together, these results provide useful elements for designing artificial transcription repressors with enhanced potency in vivo.

Oligonucleotides (ODNs) have the capacity to recognize nucleic acid targets and block the flow of genetic information at different levels (*1*, *3*). Particular attention has been dedicated to ODNs that bind to the genome and produce antigene effects in target cells (*4*−*10*). Because of this property, antigene ODNs provide a powerful therapeutic tool against viral diseases and cancer. There are, however, a number of problems that have to be solved before antigene ODNs may reach the level of clinical trials. For instance, the biological efficacy of antigene ODNs is restricted by a poor cellular uptake (*11*), ODN aggregation (*12*), susceptibility to endogenous nucleases (*13*), and, more importantly, a scarce penetration into the nucleus. To overcome these problems, several modifications of the sugar−phosphate backbone such as the replacement of a nonbridging oxygen with sulfur (*14*), the introduction of methyl (*15*) or amine groups (*16*), and restrictions to the sugar conformation (*17*) have been proposed. Among these, the sulfurization of the phosphate groups has increased significantly the ODN resistance to nucleases (*18*). To improve their cellular delivery, ODNs are generally administered entrapped in cationic liposomes. However, liposome−ODN complexes may be toxic, in particular when the phospholipids are in high excess over the ODN (*19*, *20*). Yet, positively charged liposomes may promote unspecific interaction with negatively charged plasma proteins and cellular receptors. To eliminate these obstacles, it has been recently found that cationic liposomes coated with polyethylene glycol reduce their level of interaction with biological molecules (*21*). This delivery method, however, is characterized by a low level of ODN entrapment in the coated liposomes and the difficulty of the entrapped ODN leaving the liposome interior. To improve both cellular uptake and nuclear penetration, we followed a different approach which consisted of linking covalently a chain of high-molecular mass monomethoxy polyethylene glycol (PEG)[1] to triplex-forming ODNs. PEG has been successfully used in many fields of biology for its

† Supported by FVG (LR 3/98), the University of Udine and MIUR (Cofin 2001).

* To whom correspondence should be addressed: Department of Biomedical Sciences and Technologies, School of Medicine, Piazzale Kolbe 4, 33100 Udine, Italy. Telephone: +39 0432-494395. Fax: +39 0432-494301. E-mail: lxodo@makek.dstb.uniud.it.

‡ School of Medicine.

§ Centro di Riferimento Oncologico.

|| University of Trieste.

[1] Abbreviations: DMEM, Dulbecco's modified Eagle's medium; EMSA, electrophoretic mobility shift assay; PBS, phosphate-buffered saline; PEG, polyethylene glycol; PCR, polymerase chain reaction; TBE, Tris-borate EDTA; RT, reverse transcriptase; D, duplex; T, triplex; DMS, dimethyl sulfate; HI, hexidium iodide; MTT, 3-(4,5-dimethylthiazol-2-yl)-2,5-diphenyltetrazolium bromide; PI, propidium iodide; PFA, paraformaldehyde; F, fluorescein.

10.1021/bi011314h CCC: $22.00
Published on Web 12/15/2001

Table 1: Oligonucleotides and Their Modifications Used in This Study

modified ODN	sequence	modification
bcr antigene		
ODN_{13}	5′ GGGAGGGGAAGGA	unmodified
ODN_{13}-F	5′ F-GGGAGGGGAAGGA	fluorescein
PEG ODN_{13}	5′ GGGAGGGGAAGGA-PEG	$(CH_2CH_2O)_n$
PEG ODN_{13}-F	5′ F-GGGAGGGGAAGGA-PEG	fluorescein and $(CH_2CH_2O)_n$

unique combination of biological and chemical properties. It is largely soluble in water and exhibits favorable pharmacokinetics and time distribution as well as a total lack of toxicity and immunogenicity (*22*, *23*). PEG does not inhibit Watson−Crick pairing of the linked ODN with complementary strands (*24*, *25*); it reduces the level of nonspecific interactions with endogenous proteins and is available in a wide range of molecular masses. In Table 1 are shown the ODNs and their modifications designed for this study. They are specific for a critical polypurine-polypirimidine sequence located at transcription initiation of the *bcr*/*abl* oncogene (*26*). The designed ODNs should form with the *bcr-abl* target an antiparallel triple-helical complex stabilized by A·AT and G·GC triads. The *bcr-abl* oncogene is contained in the Philadelphia (Ph) chromosome, a shortened chromosome 22 resulting from a reciprocal translocation between the long arms of chromosomes 9 and 22, t(9;22)-(q34;q11). The *bcr*/*abl* oncogene encodes a 210 kDa protein (p210) playing a key role in leukemogenesis (*27*−*29*). Protein p210 exhibits a higher tyrosine phosphokinase activity than the normal ABL protein (*27*), and its structure allows multiple protein−protein interactions, which links p210 to mitogenic and survival pathways, including the *ras* pathway (*30*). As p210 is the major causative factor in the pathogenesis of chronic myeloid leukemia (CML), an attractive therapeutic strategy should be to inhibit the expression of *bcr-abl* and/or other genes encoding downstream signal proteins. So far, attempts to reduce the intracellular level of *bcr*/*abl* mRNA through the use of antisense ODNs have been reported (*31*, *32*). An alternative approach to CML should be to downregulate the expression of the *bcr-abl* oncogene by targeting its promoter. As malignant CML cells require for their survival the expression of p210, it can be expected that the downregulation of the *bcr-abl* oncogene reduces the extent of cell proliferation. Here, we demonstrate that a 13-mer ODN conjugated to PEG (PEG ODN_{13}) (i) is taken up by Ph+ K562 and internalized in the nucleus far more efficiently than free ODN_{13}, (ii) forms a stable triple-helical complex with a critical poly(R·Y) sequence of the *bcr-abl* promoter, (iii) downregulates specifically the *bcr-abl* transcription to 65 ± 5% compared to the control, and (iv) inhibits cell growth for 32 ± 3% in a 3 day cell culture assay.

MATERIALS AND METHODS

Oligodeoxynucleotide Synthesis. The ODNs conjugated to PEG used in this study have been synthesized in liquid phase as previously described (*33*, *34*). PEG ODNs have been purified by anion exchange liquid chromatography using a Mono Q column, eluted with a linear gradient of NaCl at pH 12. The ODNs used for the footprinting experiments were synthesized in solid phase using a standard phosphoroamidite chemistry and purified by preparative 20% PAGE, in the presence of 7 M urea. The samples were lyophilized and stored at −20 °C. ODN concentrations of stock solutions in Milli Q water were determined by UV spectroscopy using as 260 nm extinction coefficients 7500, 8500, 15 000, and 12 500 M^{-1} cm^{-1} for C, T, A, and G, respectively.

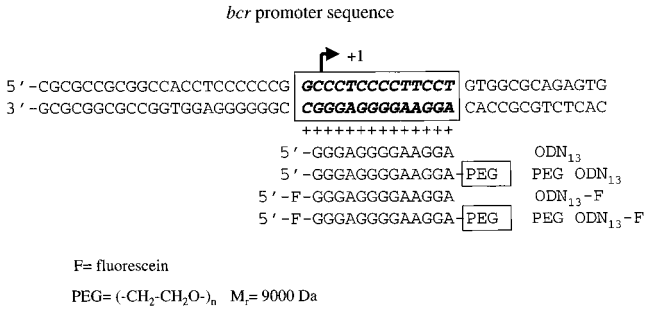

FIGURE 1: Polypurine-polypyrimidine target located in the human *bcr-abl* oncogene, at transcription initiation. The triplex-forming ODNs designed for binding to this site are shown. ODN_{13} is a nonconjugated 13-mer AG motif oligonucleotide, while PEG ODN_{13} is its isosequence analogue conjugated to a 9 kDa chain of monomethoxy polyethylene glycol. These compounds have been labeled at the 5′ end with fluorescein through an ester bond (ODN_{13}-F and PEG ODN_{13}-F). As described in ref *34*, the high-molecular mass PEG moiety has been covalently introduced onto ODN_{13} through a HELP synthetic procedure that utilizes this polymer both as a synthetic support and as a conjugating unit. The PEG-conjugated ODNs have been purified by FPLC, using a mono Q column.

Electrophoresis Mobility Shift Assay (EMSA) and Footprinting. (A) EMSA was performed using a 30-mer duplex containing the poly(R·Y) sequence of the human *bcr*/*abl* oncogene as a DNA target (Figure 1). The target was prepared by annealing (2 h at 60 °C and overnight at 37 °C) the pyrimidine strand end-labeled with [γ-^{32}P]ATP (Amersham, Pharmacia-Biotech, Milan, Italy) and polynucleotide kinase (Sigma-Aldrich, Milan, Italy) with a slight excess of the complementary purine strand. A fixed amount of labeled duplex (from 10 to 20 nM) was mixed with an excess amount of triplex-forming ODN, treated at 90 °C for 5 min, in 50 mM Tris-acetate (pH 7.4), 10 mM $MgCl_2$, and 1 ng/μL salmon sperm, and incubated at 37 °C for 3 h. After incubation, the samples were immediately run in a native 18% polyacrylamide gel (19:1 acrylamide:bisacrylamide ratio), thermostated at 4 °C to block the duplex−triplex equilibrium. The gels were dried under reduced pressure at 80 °C and analyzed on a Phosphorimager. (B) For DNase I footprinting experiments, 50-mer complementary ODNs containing the *bcr*/*abl* duplex were purified by preparative electrophoresis following a modified crush and soak method. The purine-rich strand, end-labeled with [γ-^{32}P]ATP and polynucleotide kinase, was annealed with a slight excess of the complementary pyrimidine-rich strand for 2 h at 60 °C and overnight at 37 °C. The labeled duplex (20 nM) was mixed with an excess quantity of triplex-forming ODN (5−10 μM) and incubated overnight at 37 °C in 50 mM Tris-acetate (pH 7.4) and 10 mM $MgCl_2$. Maxam and Gilbert G reactions were performed according to the standard procedure (*35*). In brief, a 50-mer target duplex (20 nM), end-labeled with [γ-^{32}P]ATP at the purine strand, was dissolved in a final volume of 20 μL containing 50 mM Tris-acetate, 10 mM $MgCl_2$, and 0.05 mg/mL salmon sperm DNA. Two microliters of 5% DMS in ethanol was added to this reaction mixture. The reaction was stopped by adding 5 μL of stop

solution [1.5 M sodium acetate (pH 7), 1 M β-mercaptoethanol, and 250 μg/mL tRNA]; the products were precipitated in 2.5 volumes of ethanol, stored for 1 h at −80 °C, and centrifuged, and the pellet was resuspended in 50 μL of a 10% piperidine solution, heated at 90 °C for 30 min, and precipitated again in 2.5 volumes of ethanol. After precipitation, the DNA was resuspended in 10 μL of gel loading buffer and heated at 90 °C. The samples were then immediately loaded in an 18% polyacrylamide gel prepared in TBE and 8 M urea, pre-equilibrated at 55 °C in a Sequi-Gen GT Nucleic Acids Electrophoresis Apparatus (Bio-Rad, Hercules, CA). After it had been run, the gel was dried and exposed to Kodak X-OMAT film.

Confocal Microscopy. Confocal microscopy experiments were performed following two staining protocols.

(A) Standard Propidium Iodide (PI) Staining of Cells Fixed on a Glass Slide. K562 cells were seeded in 12-well plates at a density of 0.8×10^5 cells in 600 μL of RPMI supplemented with 10% heat-inactivated fetal bovine serum 24 h before being added with the ODNs. Cells were treated with free ODN_{13}-F or PEG ODN_{13}-F. After centrifugation, the cells were washed twice with PBS, spun on a glass slide, and fixed with 3% paraformaldehyde (PFA) for 20 min. After the cells had been washed with 0.1 M glycine containing 0.02% sodium azide to remove PFA and Triton X-100 (0.1% in PBS), the cells were incubated with PI and RNase for 30 min at 37 °C to stain the nuclei. Then cover glasses were mounted on the glass slides with Mowiol 4-88 and Dabco (2.5%). HeLa cells were plated on a coverslip (1.2×10^5 cells in 1 mL of DMEM supplemented with 10% heat-inactivated fetal bovine serum) and grown overnight. They were then treated as described for K562 cells. K562 and HeLa cells were analyzed with a Leica DM IRBE confocal imaging system. Diaphram and fluorescence detection levels were adjusted to reduce to a minimum any interference between fluorescein and PI channels.

(B) Staining of Unfixed Live Cells with Hexidium Iodide (HI) (Molecular Probes, Eugene, OR). HI was dissolved in 1 mL of dimethyl sulfoxide to give a stock solution of 5 mg/mL which was further diluted with PBS to give a working solution of 500 μg/mL. K562 and HeLa cells were incubated with 3 μM HI for 2 h at 37 °C, washed with PBS, and grown in a medium containing PEG ODN_{13}-F or ODN_{13}-F for 6 h. After incubation, unincorporated fluorescein-labeled ODN was removed by washing with PBS, and the living cells trasferred on a glass slide were directly analyzed on the confocal microscope.

Cell Cultures. K562 human CML cells were supplied by M. Giunta (University of Udine, Udine, Italy). K562 cells were cultured in RPMI 1640 while HeLa cells in DMEM, both containing 100 units/mL penicillin, 100 μg/mL streptomycin, 200 mM L-glutamine, and 10% heat-inactivated fetal bovine serum, for 20 min at 56 °C (Celbio, Milan, Italy). KYO-1 cells were generously provided by R. E. Clark from the University of Liverpool (Liverpool, England). Cells were maintained in the logarithmic phase of growth by subculturing twice weekly.

Flow Cytometry. To study the time course of ODN uptake, K562 cells were seeded in 12-well plates at a density of 10^5 cells/600 μL. After 24 h, fluorescein-conjugated PEG ODN_{13} and free ODN_{13} were added to the cell cultures. Aliquots of the cell populations were harvested at different time intervals, spun down by centrifugation at 1000 rpm and 4 °C, washed and resuspended in PBS, and analyzed by flow cytometry. Control cells cultured in the absence of fluorescein-labeled ODN were used to set signal gain and PMT values that are necessary for assessing the fluorescence of the ODNs entrapped in the cells.

Competitive RT−PCR. To quantify the *bcr*/*abl* transcript in K562 cells, either untreated or treated with antigene effector and control molecules, we used a semiquantitative reverse trascription−polymerase chain reaction assay (C-RT−PCR) as previously decribed (*36*−*38*). cDNA was prepared from total RNA extracted from 2×10^5 K562 cells and 2×10^5 KYO-1 cells (competitor cells bearing the b2a2 *bcr*/*abl* junction) (RNAqueous-4PCR Kit, Ambion Inc., Austin, TX) in 50 μL of a reaction mixture containing 10 mM Tris-HCl (pH 8.3), 50 mM KCl, 4 mM $MgCl_2$, dATP, dCTP, dGTP, and dTTP (5 mM each) (Amersham, Pharmacia-Biotech), 25 pmol of AZ primer (CCATTTTTG-GTTTGGGCTTCACACCATTCC), 24 units of ribonuclease inhibitor, and 200 units of RT (M-MLV reverse transcriptase, Life Technologies, Milan, Italy). RT was carried out incubating the reaction mixture at 37 °C for 1 h. The *bcr*/*abl* PCR amplification was performed using 10 μL of cDNA, added with 2.5 units of DNA polymerase (AmpliTaq DNA polymerase, Perkin-Elmer, Milan, Italy) and 25 pmol of primers EA122 and EA500 (EA122, 5′ GTTTCAGAAGCTTCTC-CCTG 3′; EA500, 5′ TGTGATTATAGCCTAAGACCCG-GAG 3′), to amplify a 388 bp fragment from treated K562 cells (containing the b3a2 *bcr*/*abl* junction) and a 315 bp fragment from untreated KYO-1 cells (containing the b2a2 *bcr*/*abl* junction, competitor). In parallel, the same cDNA was used to perform a separate amplification of a 128 bp fragment of the *abl* gene (control gene). The PCR primers for *abl* were EA500 and 5′ GCTCTCGCTGGACCCAGTGA 3′ (ABL 1A), as previously described (*36*−*38*). Oligonucleotide primers were purchased from MWG-Biothec SpA (Florence, Italy). The amplification was obtained with 35 cycles (denaturation at 94 °C for 30 s, annealing at 60 °C for *bcr*/*abl* and at 55 °C for *abl* for 30 s, and extension at 72 °C for 30 s) performed on a Progene Techne (Milan, Italy) thermocycler.

RESULTS

Target Sequence and Antigene Compounds. The target of the designed triplex-forming ODNs is a critical polypurine-polypirimidine sequence located in the promoter of the human *bcr* gene, at transcription initiation (*26*) (Figure 1). In leukemia cells, the *bcr* promoter also directs the transcription of the chimeric *bcr-abl* oncogene, encoding a 210 kDa protein, which is involved in leukemogenesis (*27*−*29*). The designed ODNs are expected to bind to the poly(R·Y) target through the formation of antiparallel triple-helical complexes, stabilized by A·AT and G·GC reverse Hoogsteen base triplets (Figure 1). To enhance both cellular uptake and nuclear internalization, anti-*bcr*/*abl* ODN_{13} has been conjugated to a high-molecular mass (9000 Da) PEG chain (PEG ODN_{13}). To follow the cellular uptake, both free ODN_{13} and PEG ODN_{13} have been labeled with fluorescein via an ester linkage at the 5′ end (ODN_{13}-F and PEG ODN_{13}-F) (*39*).

PEG ODN_{13} Forms a Stable Triple Helix with the bcr/abl Target. To assay the ability of PEG ODN_{13} to bind to the

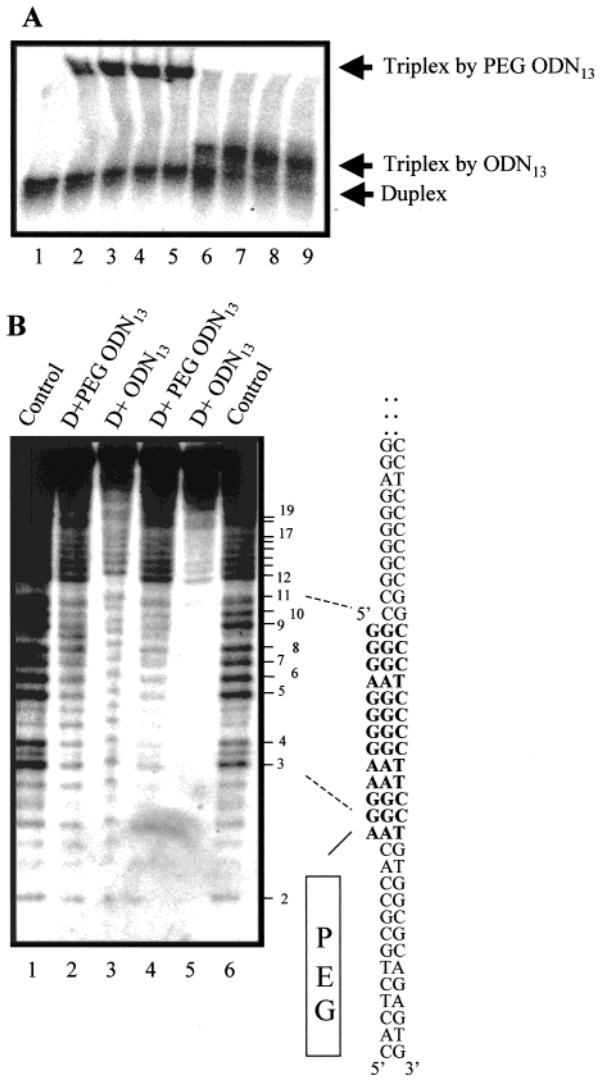

FIGURE 2: (A) Electrophoretic mobility shift assay of DNA mixtures containing the 30-mer *bcr*/*abl* duplex and triplex-forming ODN_{13} or PEG ODN_{13}. Before electrophoresis, the DNA mixtures have been incubated for 3 h at 37 °C, in 50 mM Tris-acetate (pH 7.4), 10 mM $MgCl_2$, and 1 ng/μL salmon sperm. Lane 1 shows the mobility of the 30-mer duplex (10 nM). Lanes 2−5 show the mobilities of the target duplex in the presence of increasing amounts of PEG ODN_{13} (1, 2, 5, and 10 μM, respectively). Lanes 6−9 show the mobility of the target duplex in the presence of increasing amounts of free ODN_{13} (1, 2, 5, and 10 μM, respectively). (B) DMS−piperidine footprinting of a 50-mer target duplex incubated with PEG ODN_{13} and free ODN_{13} at 37 °C in 50 mM Tris-acetate, 10 mM $MgCl_2$ (pH 7.4), and 1 ng/μL salmon sperm. Lanes 1 and 6 show DMS modification of the *bcr*/*abl* target in the presence of a random sequence ODN (10 μM) that is unable to form a triplex with the target (lane 1) or PEG (lane 6). Lanes 2−5 show that both ODN_{13} and PEG ODN_{13} bind to the target and protect the expected region comprised of guanines 3−11. The concentrations of ODN_{13} (lanes 3 and 5) and PEG ODN_{13} (lanes 2 and 4) are 5 and 10 μM, respectively.

bcr/*abl* target, we first conducted electrophoresis mobility shift experiments (EMSA). To this end, a 30-mer duplex containing the *bcr-abl* target was end-labeled with T4 polynucleotide kinase and [γ-^{32}P]ATP, mixed with increasing amounts of either free ODN_{13} or PEG ODN_{13}, and incubated for 3 h at 37 °C in 50 mM Tris-acetate (pH 7.4) and 10 mM $MgCl_2$. Figure 2A shows the electrophoretic profiles obtained with the DNA mixtures. It can be seen that both free ODN_{13} and PEG ODN_{13} slow the mobility of the 30-mer target duplex, but the latter in a more dramatic way than the former, as PEG markedly increases the frictional coefficient of PEG ODN_{13}. At 37 °C and pH 7.4, we roughly estimated dissociation constants (K_d) that were between 10^{-6} and 10^{-7} M, on the basis of the equation $[D]/[T] = K_d(1/[\text{PEG ODN}_{13}])$, where [D]/[T] is the ratio of the duplex (D) to the triplex (T), while [PEG ODN_{13}] is the equilibrium concentration of PEG ODN_{13} or ODN_{13} which is approximately equal to their initial concentration, as they have been used in large excess over the target. As observed for duplex formation (*24*, *25*), EMSA data showed that PEG conjugation also has little effect on triplex formation.

The binding of PEG ODN_{13} to the *bcr*/*abl* target was also analyzed by DMS−piperidine footprinting, conducted at 37 °C in 50 mM Tris-acetate (pH 7.4) and 10 mM $MgCl_2$ (Figure 2B). It should be remembered that DMS reacts with guanine N7 when this base is not involved in reverse Hoogsteen hydrogen bonding to the third strand. Lane 1 shows the results of DMS modification of the 50-mer target duplex, in the presence of a 20-mer G-rich random sequence ODN (control). As the guanines of the *bcr*/*abl* target (numbered from 1 to 19) are not involved in hydrogen bonding, they give rise to an equal number of intense bands. Lane 6 shows the DMS−piperidine reaction conducted in the presence of PEG (control). Strong inhibition of DMS guanine modification is observed in lanes 2−5 where the reactions were performed on the *bcr*/abl 50-mer duplex mixed with either PEG ODN_{13} (lanes 2 and 4) or free ODN_{13} (lanes 3 and 5). Note that in lanes 3 and 5 at the 3′ end of the target, the G bases, numbered from 12 to 17, appears to be slightly protected, probably because a complex with a 2:1 ODN_{13}:D stoichiometry is formed by free ODN_{13} and the *bcr*/*abl* target:

```
5′-ACCTCCCCCCGGCCCTCCCCTTCCTGTGGCGCA
3′-TGGAGGGGGGCCGGGAGGGGAAGGACACCGCGT
     GGAGGGGAA   GGGAGGGGAAGGA
5′G                      GGA
```

This complex, however, does not seem to form with PEG ODN_{13}, probably because the 3′ PEG chain hinders binding to the secondary site.

Effect of PEG on Nuclease ODN Degradation. To investigate whether PEG confers resistance to anti-*bcr*/*abl* ODNs against nuclease degradation, both free ODN_{13} and PEG ODN_{13}, labeled with ^{32}P, were exposed to S1 (0.15 unit) or fetal bovine serum (80%) for increasing incubation times**.** After incubation, the DNA mixtures were frozen at −80 °C to block the enzyme reaction and successively analyzed in a denaturing (7 M urea) 16% polyacrylamide gel. The amounts of intact ODN and degradation products were determined by measuring the intensity of their electrophoretic bands with a LKB Ultrascan XL enhanced laser densitometer. The results are reported in Figure 3A as the percentage of residual nondegraded ODN as a function of time. It can be seen that free ODN_{13} is degraded more rapidly than PEG ODN_{13}, at all incubation times that were considered, in keeping with previous results obtained with ODNs conjugated to PEG at both the 3′ and 5′ ends (*24*). To rationalize this behavior, one can assume that the 3′ PEG chain may reduce the affinity of PEG ODN_{13} for the nucleases.

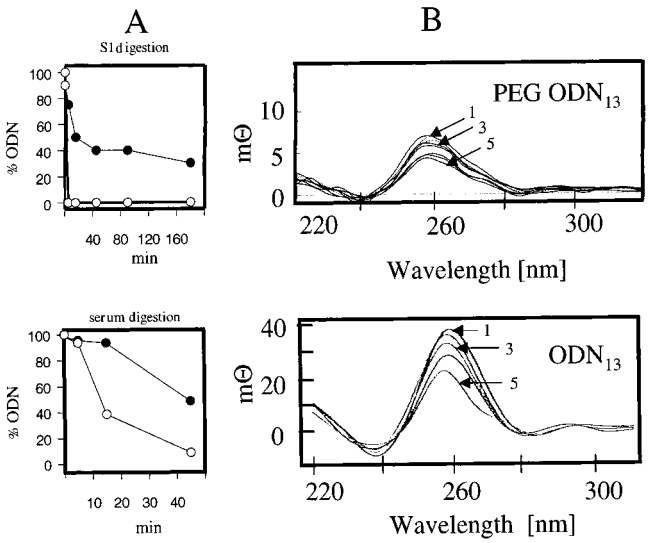

FIGURE 3: (A) Digestion of ODN_{13} and PEG ODN_{13} by nuclease S1 (top) and blood serum (bottom). Black circles depict data for PEG ODN_{13}, while white circles depict data for ODN_{13}. The ordinate reports the percent residual nondegraded ODN as determined from electrophoresis. (B) Circular dichroism spectra as a function of temperature of free ODN_{13} and PEG ODN_{13} in 50 mM Tris-acetate and 10 mM $MgCl_2$ (pH 7.4). The CD signal in the ordinate is expressed as mΘ; spectra have been obtained from a 3 μM solution in a 0.5 path length quartz cuvette. Spectra 1, 3, and 5 for both oligonucleotides have been obtained by setting the cuvette holder temperature at 25, 50, and 80 °C, respectively. The other spectra shown in the figure have been recorded at intermediate temperatures.

We also investigated by circular dichroism spectroscopy whether anti-*bcr*/*abl* PEG ODN_{13} and free ODN_{13} self-associated in solution, as both are composed of a guanine-rich sequence (*12*). Figure 3B shows that 2 μM PEG ODN_{13} is characterized by a weak positive ellipticity at 260 nm (~8 mΘ), while 3 μM free ODN_{13} exhibits a 4-fold stronger ellipticity (~35 mΘ), whose intensity decreased significantly with temperature. Such behavior suggests that PEG ODN_{13} does not exhibit or hardly exhibits self-association in solution, while free ODN_{13} clearly self-associates (*40*, *41*).

Uptake and Nuclear Internalization As Studied by Microscopy. Cellular uptake studies have been performed on suspension-growing K562 cells and adhesion-growing HeLa cells, following two different staining procedures. In one case, we followed a standard method based on fixing the cells on a glass slide after incubation with free ODN_{13}-F or PEG ODN_{13}-F, with subsequent exposure to 0.1% Triton X-100 and PI. As Triton X-100 permeabilizes the cell membrane, it is possible that some oligonucleotides taken up by the cells become lost during the washing steps. For this reason, we also stained directly the cells with HI, a dye that binds to DNA and RNA in live cells and displays red fluorescent light (*42*). In this case, HeLa and K562 cells were treated for 2 h with HI, transferred in a medium containing either free ODN_{13}-F or PEG ODN_{13}-F, and left to grow for a certain time, and then they were analyzed on the confocal microscope.

Figure 4A shows the images obtained with fixed K562 cells stained with PI. Panel A shows the nuclei of two cells stained with PI (red light); panel B shows the intracellular distribution of PEG ODN_{13}-F (green light), while panel C displays a superimposed view of the red and green fluorescence lights, showing that PEG ODN_{13}-F is present in both the cytoplasm and the nucleus (orange/yellow light). To further confirm that PEG ODN_{13} was internalized in the nucleus, we performed vertical sections along the *z*-axis. A typical *z*-section is reported in panel Z. Panels D−F show the images obtained by delivering free ODN_{13}-F to the K562 cells. No green light was observed, suggesting that ODN_{13}-F

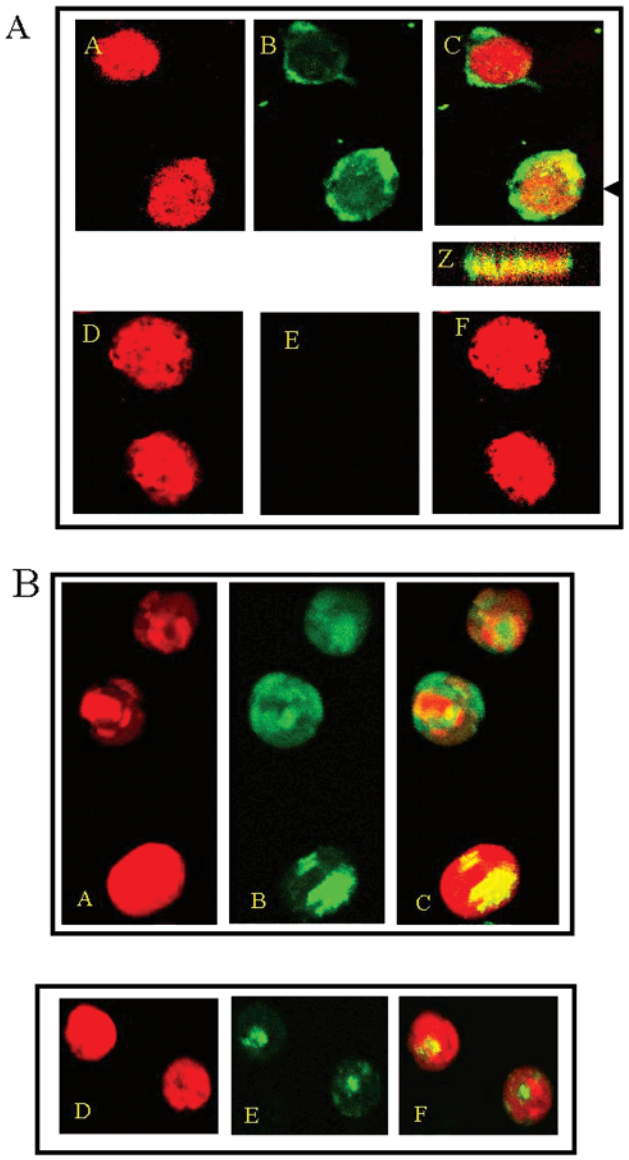

FIGURE 4: (A) Confocal images of K562 cells exposed for 6 h to 10 μM PEG ODN_{13} (A−C) and free ODN_{13}-F (D−F). After incubation, the cells were cytospinned on a glass slide, fixed with 3% PFA, stained with PI, and analyzed by confocal microscopy (Leica confocal laser scanning system equipped with Cosmos software). Cell nuclei have been stained with PI which emits red fluorescent light upon excitation at 543 nm (A). Fluorescein-labeled ODN_{13}-F and PEG ODN_{13}-F are detected by exciting fluorescein at 488 nm (B). Panel C shows a superimposed view of the red and green emissions. Each image is the projection of eight *z*-axis sections. Note that the presence of the PEG ODN_{13} in the nucleus is visualized by the yellow light. Panels D−F show confocal images of ODN_{13}-F administered to the cells as a free molecule, i.e., without a carrier. A vertical *z*-axis plane section of a cell treated with PEG ODN_{13} is shown in panel Z. (B) Confocal images of unfixed live K562 cells growing in suspension in RPMI and stained with HI. Panels A−C show K562 cells treated with PEG ODN_{13}, and panels D−F show K562 cells treated with ODN_{13}.

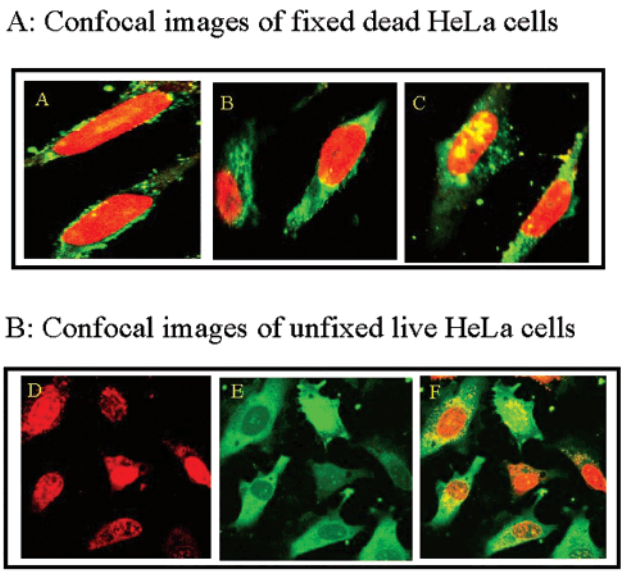

FIGURE 5: (A) Confocal images obtained with fixed HeLa cells stained with PI exposed for 12 h to PEG ODN_{13}-F at three different concentrations: 2.5 (A), 5 (B), and 10 μM (C). (B) Confocal images of unfixed HeLa cells stained with HI and exposed to 3 μM PEG ODN_{13} for 12 h.

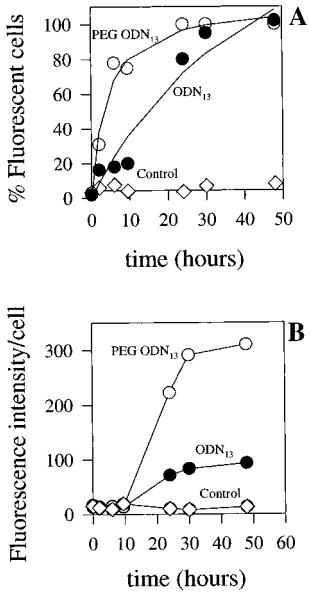

FIGURE 6: (A) Percent fluorescent K562 cells exposed to 10 μM PEG ODN_{13}-F (○) or 10 μM ODN_{13}-F (●) as a function of time. The control is untreated cells (◇). (B) Average fluorescent intensity per cell after treatment with 10 μM ODN_{13}-F or 10 μM PEG ODN_{13}-F. The data were obtained via flow cytometry.

was hardly taken up by the cells. Figure 4B shows images obtained from unfixed live K562 cells growing in suspension. Panel A shows the cells stained with HI. As this dye binds to DNA and RNA, it stains both the nucleus and the cytoplasm. Panel B shows the green fluorescence emitted by PEG ODN_{13}-F which was taken up by the cells, while panel C shows a superimposed view of panels A and B. These images clearly demonstrate that PEG ODN_{13} has the capacity to penetrate intact cells that are alive and growing in the liquid culture medium. Curiously, a nonhomogeneous but "clumpy" cellular distribution of both HI and PEG ODN_{13}-F was observed (*43*). For this behavior, the superimposed views gave rise to areas stained in orange, green, and yellow. In contrast with the PI staining, this technique clearly showed that a small fraction of free ODN_{13}-F was also able to penetrate K562 cells (panels D−F).

Figure 5A shows the uptake of PEG ODN_{13}-F by HeLa cells, exposed for 6 h to 2.5, 5, and 10 μM PEG ODN_{13}-F, fixed on glass, and stained with PI. Note that at all the concentrations that were used PEG ODN_{13}-F is located in both the cytoplasm and the nuclei. Figure 5B shows the images obtained with unfixed HeLa cells stained with HI. The confocal images clearly show that all cells have taken up a large quantity of PEG ODN_{13}-F. We also sought to determine whether the level of uptake by K562 and HeLa cells of free ODN_{13} delivered with Dotap (a cationic liposome) increased. We found that Dotap enhanced significantly the uptake of free ODN_{13}-F, but produced in the cell nuclei large vescicles apparently filled with oligonucleotide (not shown).

Time Course of PEG ODN_{13}-F Uptake. The fluorescence associated with K562 cells exposed to PEG ODN_{13}-F and free ODN_{13}-F was measured by flow cytometry. Figure 6 (top) shows the percentage of fluorescent cells as a function of incubation time. These curves show that PEG increases the rate at which the cells exposed to PEG ODN_{13}-F become fluorescent compared to the rate of the cells exposed to free ODN_{13}-F. The incubation time required to obtain 50% of fluorescent cells is 18 and 2.5 h for free ODN_{13}-F and PEG ODN_{13}-F, respectively. In Figure 6B is reported the average fluorescence intensity per cell obtained with free ODN_{13}-F and PEG ODN_{13}-F at increasing incubation times. It can be seen that after incubation for 48 h, PEG ODN_{13}-F promoted an average fluorescence intensity per cell that was ~5-fold higher than that obtained with the cells treated with free ODN_{13}-F.

PEG ODN_{13} Inhibits Cell Growth and Downregulates bcr/abl Transcription. Proliferation assays of K562 cells cultured in the presence of 15 μM PEG ODN_{13}, free ODN_{13}, or control molecules were performed using the tetrazolium MTT salt (*44*). We obtained growth curves covering an incubation period of up to 72 h, which reported on the ordinate the ratio (*T*/*C*) between treated (*T*) and untreated (*C*) cells as a function of incubation time (Figure 7). It was found that free ODN_{13} (■) did not have any antiproliferative effect on K562 cells while PEG ODN_{13} (○) produced a growth inhibitory effect of 22 ± 3% compared to untreated cells, and 32 ± 3% compared to cells treated only with PEG (●). In contrast, K562 cells treated with PEG RDN, a PEG-conjugated random sequence ODN, did not have a significant effect on cell growth (◇).

The level of *bcr*/*abl* mRNA present in the cells after being exposed to anti-*bcr*/*abl* ODNs for 24 and 48 h has been measured by competitive RT−PCR (semiquantitative method), as previously described (*36*−*38*). We found that after incubation for 24 h in the presence of PEG ODN_{13} the level of *bcr*/*abl* mRNA in K562 cells was downregulated at 80% compared to the control. A higher level of transcription inhibition was observed in a 48 h cell culture assay, in which PEG ODN_{13} downregulated the transcription of *bcr*/*abl* at 65 ± 5% with respect to control (Figure 8). As a control, we have measured in the same cDNA sample the level of *abl* mRNA by RT−PCR and found that no inhibition was promoted either by ODN_{13} or by PEG ODN_{13}. It can be seen

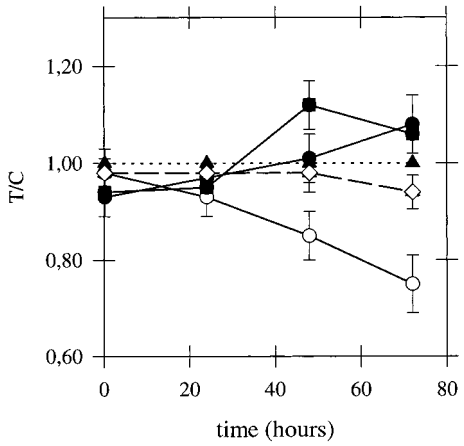

FIGURE 7: Growth curves covering a 3 day incubation period determined by the MTT assay. The data are expressed in terms of *T*/*C* (OD of treated cells/OD of control cells) as a measure of cell viability and survival in the presence of the test oligonucleotide. Curves depict data for (●) cells treated with PEG (control), (■) cells treated with free ODN_{13}, (▲) untreated cells (control), (◇) cells treated with PEG RDN, a 12-mer G-rich random sequence ODN conjugated to PEG (control), and (○) cells treated with antigene PEG ODN_{13}.

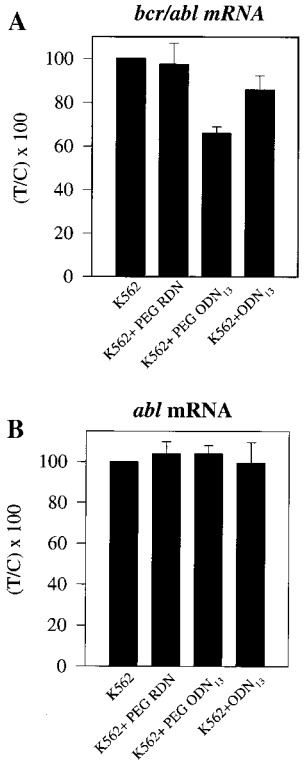

FIGURE 8: (A) Relative level of *bcr*/*abl* mRNA in treated K562 cells measured by a semiquantitative method based on competitive RT−PCR as previously described (*36*−*38*). The histograms depict values of (*T*/*C*) × 100, where *T* is the ratio between *bcr*/*abl* mRNA from treated K562 cells and *bcr*/*abl* mRNA from untreated KYO-1 cells (competitor) while *C* is the ratio between mRNA from untreated K562 and KYO-1 cells. PEG RDN is a 12-mer G-rich random sequence ODN conjugated to PEG used as control. (B) Relative level of *abl* mRNA in treated and untreated K562 cells measured by competitive RT−PCR. The histograms depict values of (*T*/*C*) × 100.

also that free ODN_{13} seems to produce a slight inhibitory effect, in keeping with its lower capacity to penetrate cell membranes.

DISCUSSION

In our efforts to design artificial transcription repressors for antigene strategies, we explored in this study the possibility of conjugating a high-molecular mass PEG chain to a 13-mer AG motif triplex-forming ODN specific for a critical poly(R·Y) sequence located at the transcription initiation site of the chimeric *bcr-abl* oncogene contained in Ph+ leukemia cells. Band-shift and footprinting studies demonstrated that 9000 Da PEG does not inhibit the capacity of anti-*bcr* PEG ODN_{13} to bind to its correspondent target through the formation of a stable triple helix. The dissociation equilibrium constant K_d for PEG ODN_{13} measured at 37 °C and pH 7.4 was between 10^{-6} and 10^{-7} M. Previous studies have reported that neither low- nor high-molecular mass PEG chains coupled to ODNs affect duplex formation (*24*, *25*). Footprinting experiments show that both PEG ODN_{13} and free OND_{13} protect the region of the target to which it is expected to bind, suggesting that the PEG chain linked to the ODN 3′ end neither interacts with the double helix of the DNA target nor promotes unspecific binding.

One interesting result of this study is that PEG conjugation markedly enhanced the ODN cellular uptake in both types of cells that were considered. Confocal laser microscopy showed that fluorescein-labeled PEG ODN_{13} was far more efficiently taken up and internalized in the nuclei by K562 and HeLa cells than the nonconjugated isosequence free ODN_{13}. This important feature for antigene molecules has been detected not only following a standard PI staining technique but also direcly on live cells stained with HI, a dye binding to RNA and DNA in vivo. In addition, flow cytometry measurements showed that the average fluorescence intensity assumed by K562 cells exposed to PEG ODN_{13} was ∼5-fold higher than that observed in K562 cells exposed to free ODN_{13}. The capacity of PEG to increase the level of cellular uptake has recently been demonstrated by coating several cationic liposomes, which were used for delivering ODN to cells, with PEG (*21*). It was reported that PEG (2000 Da)-modified cationic liposomes enhanced from 4- to 13-fold the cellular delivery mediated by cationic liposomes. However, this delivery method suffered from a low efficiency of the entrapped ODN leaving the interior of the cationic liposome. In our case, the problems arising from the use of cationic liposomes are avoided, as the carrier driving the ODN into the cell is a neutral chain of PEG covalently linked to the ODN itself. In addition, it is known that the use of a cationic liposome for transfecting DNA into cells is limited by cytotoxic problems (*45*).

We found that PEG ODN_{13} impaired the growth of K562 cells for ∼32 ± 3% in a 3 day culture assay, compared to cells treated with only PEG or PEG RDN. Activity was observed at 15 μM, and an antigene mechanism was involved as PEG ODN_{13} promoted a downregulation of *bcr*/*abl* mRNA transcription at 65 ± 5% with respect to control. The results of this study suggest that the biological effect observed with PEG ODN_{13} on *bcr*/*abl* expression can be attributed to the PEG chain that not only enhances the cellular uptake and nuclear internalization but also increases the intracellular stability of the PEG-conjugated ODN.

Triplex-forming PEG ODN_{13} is directed against the initiation element of the *bcr*/*abl* gene, a C- and G-rich region that lies over the transcription start site (*26*). This critical

region, 40 nucleotides downstream from the TATA box, interacts with the transcription machinery to promote transcription initiation. It is therefore reasonable to expect that PEG ODN_{13} hinders the binding of nuclear factors and/or RNA polymerase II to the initiation element.

In view of these results, we addressed the question of whether there is a link between the observed cell growth inhibition and the downregulation of the *bcr*/*abl* oncogene. A number of studies suggest that protein p210, the product of the *bcr*/*abl* oncogene, activates mitogenic pathways and confers a growth advantage of Ph+ cells over normal hematopoietic cells (*27*−*30*). In particular, it seems that p210 through the interaction with adaptor proteins activates constitutively the *ras* pathway which promotes cell proliferation in leukemia cells. Thus, the observation that PEG ODN_{13} impairs cell growth can be rationalized in terms of antigene activity against the *bcr*/*abl* oncogene. There are also data supporting the notion that the *bcr*/*abl* protein is involved in survival signals. For instance, *bcr-abl* positive cells are resistant to apoptosis induced by DNA damage (*30*, *46*). The biological mechanism is not yet well understood; however, there is evidence that the *bcr*/*abl* protein prevents apoptosis by activating the *bcl-2* gene (*27*). Therefore, the inhibition of p210 expression by PEG ODN_{13} might expose the cells to apoptosis. In keeping with this rationale, we have observed by confocal microscopy that a significant number of K562 cells exposed to PEG ODN_{13} exhibited fragmentation of the nucleus, typical of apoptosis (not shown).

In conclusion, our data provide evidence that PEG ODN_{13} designed specifically for a critical poly(R•Y) tract located in the 5′ region of the *bcr*/*abl* oncogene is able to downregulate *bcr*/*abl* mRNA at 65 ± 5% with respect to control and to inhibit cell growth by 32 ± 3% in 3 day liquid culture assays. The advantage of PEG-conjugated ODNs over isosequence free ODNs can be ascribed to the fact that the former easily penetrate the cell membranes, are internalized in the nucleus, and undergo little self-aggregation in solution. We believe that a stronger antiproliferative effect on Ph+ cells will be obtained by synthesizing PEG ODNs longer than 13 nucleotides with more affinity for the *bcr* target (*47*), containing some thioate groups to further enhance nuclease resistance (*48*). Work in this direction is in progress in our laboratories.

ACKNOWLEDGMENT

We thank Prof. A. Colombatti (Centro di Riferimento Oncologico) for the use of the confocal microscope.

REFERENCES

1. Chang, P. P., and Glazer, P. M. (1997) *J. Mol. Med. 75*, 267−282.
2. Praseuth, D., Guieysse, A. L., and Hélène, C. (1999) *Biochim. Biophys. Acta 1489*, 181−206.
3. Vasquez, K., and Wilson, J. (1996) *Trends Biol. Sci. 23*, 4−9.
4. McShan, W. M., Rossen, R. D., Laughter, A. H., Trial, J., Kesseler, D. J., Zendegui, J. G., Hogan, M. E., and Orson, F. M. (1992) *J. Biol. Chem. 267*, 5712−5721.
5. Kovacs, A., Kandala, J. C., Weber, K. T., and Guntaka, R. V. (1996) *J. Biol. Chem. 271*, 1805−1812.
6. Alunni-Fabbroni, M., Pirulli, D., Manzini, G., and Xodo, L. (1996) *Biochemistry 35*, 16361−16369.
7. Kim, H. G., Reddoch, J. F., Mayfield, C., Eddinghaus, S., Vigneswaran, N., Thomas, S., Jones, D. E., and Miller, D. M. (1998) *Biochemistry 37*, 2299−2304.
8. Cogoi, S., Suraci, C., del Terra, E., Diviacco, S., van der Marel, G., van Boom, J., Quadrifoglio, F., and Xodo, L. (2000) *Antisense Nucleic Acid Drug Dev. 10*, 283−295.
9. Faria, M., Wood, C. D., Perrouault, L., Nelson, J. S., Winter, A., White, M. R., Helene, C., and Giovannangeli, C. (2000) *Proc. Natl. Acad. Sci. U.S.A. 97*, 3862−3867.
10. Morasustti, C., Scaggiante, B., Xodo, L. E., Dapas, B., Paroni, G., Tolazzi, G., and Quadrofoglio, F. (1999) *Antisense Nucleic Acid Drug Dev. 9*, 261−270.
11. Nagel, K. M., Holstad, S. G., and Isenberg, K. E. (1993) *Pharmacotherapy 13*, 177−188.
12. Cheng, A. J., Wang, J. C., and Van Dyke, M. W. (1998) *Antisense Nucleic Acid Drug Dev. 8*, 215−225.
13. Agrawal, S. (1996) *Trends Biotechnol. 14*, 376−378.
14. Stein, C. A., Subasinghe, C., Shinozuka, K., and Cohen, J. S. (1988) *Nucleic Acids Res. 16*, 3209−3221.
15. Miller, P. S. (1991) *Biotechnology 9*, 358−362.
16. Froehler, B. N., and Matteucci, M. (1988) *Nucleic Acids Res. 16*, 4831−4839.
17. Sanghvy, Y. S., and Cook, P. D. (1994) in *Carbohydrate modification in antisense research* (Sanghvi, Y. S., and Cook, P. D., Ed.) American Chemical Society, Washington, DC.
18. Eckstein, F. (2000) *Antisense Nucleic Acid Drug Dev. 10*, 117−121.
19. Zelphati, O., and Szoka, F. C., Jr. (1996) *Pharm. Res. 13*, 1367−1372.
20. Zelphati, O., and Szoka, F. C., Jr. (1996) *Proc. Natl. Acad. Sci. U.S.A. 93*, 11493−11498.
21. Meyer, O., Kirpotin, D., Hong, K., Sternberg, B., Park, J. W., Woodlwe, M. C., and Papahadjopoulos, D. (1998) *J. Biol. Chem. 273*, 15621−15627.
22. Tsutsumi, Y., Onda, M., Nagata, S., Lee, B., Kreitman, R. J., and Pastan, I. (2000) *Proc. Natl. Acad. Sci. U.S.A. 97*, 8548−8553.
23. Mehvar, R. (2000) *J. Pharm. Pharm. Sci. 3*, 125−136.
24. Jäschke, A., Furste, J. P., Nordhoff, E., Hillenkamp, F., Cech, D., and Erdmann, V. A. (1994) *Nucleic Acids Res. 22*, 4810−4817.
25. Vorobjev, P. E., Zarytova, V. F., and Bonora, G. M. (1999) *Nucleosides Nucleotides 18*, 2745−2750.
26. Zhu, Q. S., Heisterkamp, N., and Groffen, J. (1990) *Nucleic Acids Res. 18*, 7119−7125.
27. Deininger, M. W. N., Goldman, J. M., and Melo, J. V. (2000) *Blood 96*, 3343−3356.
28. Faderl, S., Talpaz, M., Estrov, Z., O'Brien, S., Kurzrock, R., and Kantarjian, H. M. (1999) *N. Engl. J. Med. 341*, 164−172.
29. Warmuth, M., Danhauser-Riedl, S., and Hallek, M. (1999) *Ann. Hematol. 78*, 49−64.
30. Sanchez-Garcia, I., and Martin-Zanca, D. (1997) *J. Mol. Biol. 267*, 225−228.
31. Skorski, T., Nieborowska-Skorska, M., Nicolaides, N. C., Szczylik, C., Iversen, P., Iozzo, R. V., Zon, G., and Calabretta, B. (1994) *Proc. Natl. Acad. Sci. U.S.A. 91*, 4504−4508.
32. Rowley, P. T., Kosciolek, B. A., and Kool, E. T. (1999) *Mol. Med. 5*, 693−700.
33. Bonora, G. M., Ivanova, E., Zarytova, V., Burcovich, B., and Veronese, F. M. (1997) *Bioconjugate Chem. 8*, 793−797.
34. Bonora, G. M. (1995) *Appl. Biochem. Biotechnol. 54*, 3−17.
35. Sambrook, J., Fritsch, E. F., and Maniatis, T. (1989) *Molecular Cloning: A Laboratory Manual*, Cold Spring Harbor Laboratory Press, Plainview, NY.
36. Moravcova, J., Lukasova, M., Stary, J., and Haskovec, C. (1998) *Leukemia 12*, 1303−1312.
37. Malinge, M. C., Mahon, F. X., Delfau, M. H., Daheron, L., Kitzis, A., Guilhot, F., Tanzer, J., and Grandchamp, B. (1992) *Br. J. Haematol. 82*, 701−703.
38. van Rhee, F., Marks, D. I., Lin, F., Szydlo, R. M., Hochhaus, A., Treleaven, J., Delord, C., Cross, N. C., and Goldman, J. M. (1995) *Leukemia 9*, 329−335.

39. Ballico, M., Drioli, S., Morvan, F., Rapozzi, V., Xodo, L. E., and Bonora, G. M. (2001) *Bioconjugate Chem. 12*, 719−725.
40. Rhodes, D., and Giraldo, R. (1995) Telomere structure and function, *Curr. Opin. Struct. Biol. 5*, 311−322.
41. Hardin, C. C., Henderson, E., Watson, T., and Prosser, J. K. (1991) *Biochemistry 30*, 4460−4472.
42. Haughland, R. P. (1996) in *Handbook of fluorescent probes and research chemicals, Nucleic acid detection* (Spence, M. T. Z., Ed.) pp 143−168, Molecular Probes, Eugene, OR.
43. Cutrona, G., Carpeneto, E. M., Ulivi, M., Roncella, S., Landt, O., Ferrarini, M., and Boffa, L. C. (2000) *Nat. Biotechnol. 18*, 300−303.
44. Mosmann, T. (1983) *J. Immunol. Methods 65*, 55−63.
45. Roche Diagnostics GmbH, Roche Molecular Biochemicals (1999) *DOTAP Liposomal transfection reagent*, version 3, Mannheim, Germany.
46. Bedi, A., Zehnbauer, B. A., Barbers, J. P., Sharkis, S. J., and Jones, R. J. (1994) *Blood 83*, 2038−2044.
47. Xodo, L., Thenmalarchelvi, R., Quadrifoglio, F., Manzini, G., and Yathindra, N. (2001) *Eur. J. Biochem. 268*, 656−664.
48. Cogoi, S., Rapozzi, V., Quadriofoglio, F., and Xodo, L. E. (2001) *Biochemistry 40*, 1135−1143.

BI011314H